Short-range incommensurate magnetic order near the superconducting phase boundary in $Fe_{1+\delta}Te_{1-x}Se_x$

Jinsheng Wen,[1,2] Guangyong Xu,[1] Zhijun Xu,[1,3] Zhi Wei Lin,[1] Qiang Li,[1] W. Ratcliff,[4] Genda Gu,[1] and J. M. Tranquada[1]
[1]*Condensed Matter Physics and Materials Science Department, Brookhaven National Laboratory, Upton, New York 11973, USA*
[2]*Department of Materials Science and Engineering, Stony Brook University, Stony Brook, New York 11794, USA*
[3]*Physics Department, The City College of New York, New York, New York 10031, USA*
[4]*NIST Center for Neutron Research, National Institute of Standards and Technology, Gaithersburg, Maryland 20899, USA*
(Received 19 June 2009; revised manuscript received 6 August 2009; published 10 September 2009)

We performed elastic neutron-scattering and magnetization measurements on $Fe_{1.07}Te_{0.75}Se_{0.25}$ and $FeTe_{0.7}Se_{0.3}$. Short-range incommensurate magnetic order is observed in both samples. In the former sample with higher Fe content, a broad magnetic peak appears around (0.46,0,0.5) at low temperature, while in $FeTe_{0.7}Se_{0.3}$, the broad magnetic peak is found to be closer to the antiferromagnetic (AFM) wave vector (0.5,0,0.5). The incommensurate peaks are only observed on one side of the AFM wave vector for both samples, which can be modeled in terms of an imbalance of ferromagnetic/antiferromagnetic correlations between nearest-neighbor spins. We also find that with higher Se (and lower Fe) concentration, the magnetic order becomes weaker while the superconducting temperature and volume increase.

DOI: 10.1103/PhysRevB.80.104506 PACS number(s): 61.05.fg, 74.70.Dd, 75.25.+z, 75.30.Fv

Since the recent discovery of Fe-based superconductors with high critical temperatures (T_c),[1–4] extensive research has been carried out to study the magnetic structures in these materials[5–7] as magnetic fluctuations are expected to play an important role in producing the unconventional superconductivity.[8–10] It is now well established that in LaFeAsO-(1:1:1:1) (Refs. 11–13) and $BaFe_2As_2$-(1:2:2) (Refs. 14–17) type compounds, the long-range magnetic order is suppressed with doping, while the superconductivity appears above a certain doping value. While there are some rare cases where superconductivity appears sharply after magnetic order disappears,[12] in most systems short-range magnetic order coexists with superconductivity over some range of doping.[11,13–17]

In the more recently discovered system $Fe_{1+\delta}Te_{1-x}Se_x$ (1:1),[18–20] it is found that (i) long-range magnetic order is present in nonsuperconducting $Fe_{1+\delta}Te$,[21–23] but only short-range magnetic order survives in superconducting samples with 33% (Ref. 23) and 40% Se (Ref. 20); (ii) the observed magnetic order has a different propagation wave vector from that of the other Fe-based systems. To describe the ordering, we consider a tetragonal unit cell containing two Fe atoms per plane and specify wave vectors in reciprocal-lattice units (r.l.u.) of $(a^*,b^*,c^*)=(2\pi/a,2\pi/b,2\pi/c)$; the unit cell is rotated 45° in the *a*-*b* plane from that used for 1:1:1:1 and 1:2:2 systems.[22] In the latter systems, the spin-density-wave (SDW) order is commensurate with propagation wave vector (0.5,0.5,0.5), generally attributed to nesting of the Fermi surface.[22,24–26] In the 1:1 system, the SDW order propagates along (0.5,0,0.5) and can be either commensurate or incommensurate depending on the Fe content.[22,23] Calculations using the local spin-density approximation for hypothetical stoichiometric FeTe yield a commensurate magnetic ground state consistent with that seen experimentally;[27,28] however, the (0.5,0.5,0.5) SDW order is calculated to have the lowest energy for FeSe.[27]

To address the evolution of the magnetic correlations with Se concentration, we have performed elastic neutron-scattering and magnetization measurements on high-quality single crystals with different Fe and Se contents. We show that there is short-range incommensurate magnetic order in both $Fe_{1.07}Te_{0.75}Se_{0.25}$ and $FeTe_{0.7}Se_{0.3}$ at low temperature. Broad magnetic peaks appear at positions slightly displaced from the antiferromagnetic (AFM) wave vector (0.5,0,0.5) in both samples when cooled below $\lesssim 40$ K. The peak intensity increases with further cooling and persists into the superconducting phase. The magnetic peak intensity drops with more Se and less Fe content and with strengthening superconductivity.

Single crystals with nice (001) cleavage planes were grown by a unidirectional solidification method with nominal compositions of $Fe_{1.07}Te_{0.75}Se_{0.25}$ and $FeTe_{0.7}Se_{0.3}$ and respective masses of 4.7 and 7.2 g. Neutron scattering experiments were carried out on the triple-axis spectrometer BT-9 located at the NIST Center for Neutron Research. The scattering plane (*H*0*L*) is defined by two vectors [100] and [001] in tetragonal notation. The lattice constants for both samples are $a=b=3.80(8)$ Å and $c=6.14(7)$ Å.

The bulk magnetization was characterized using a superconducting quantum interference device (SQUID) magnetometer. In the magnetization measurements, each sample was oriented so that the (001) plane was parallel to the magnetic field. The zero-field-cooling (ZFC) magnetization vs. temperature for each sample is shown in Fig. 1(a), where one can see that the 25% Se sample only shows a trace of superconductivity, while the 30% Se sample clearly has a $T_c \sim 13$ K. We estimate that the superconducting volume fraction for the latter sample is ~1%. The inset of Fig. 1(a) shows that the paramagnetic magnetization grows on cooling and is greater in the sample with less Se (and more Fe). The paramagnetic response does not follow simple Curie-Weiss behavior, so it is not possible to make a meaningful estimate of effective magnetic moments. For the 25% Se sample, there is a shoulder at ~60 K which could be due to 2%–3% of $Fe_{1+\delta}Te$ as a second phase, which has a magnetic phase transition temperature of ~65 K.[22]

 ©2009 The American Physical Society

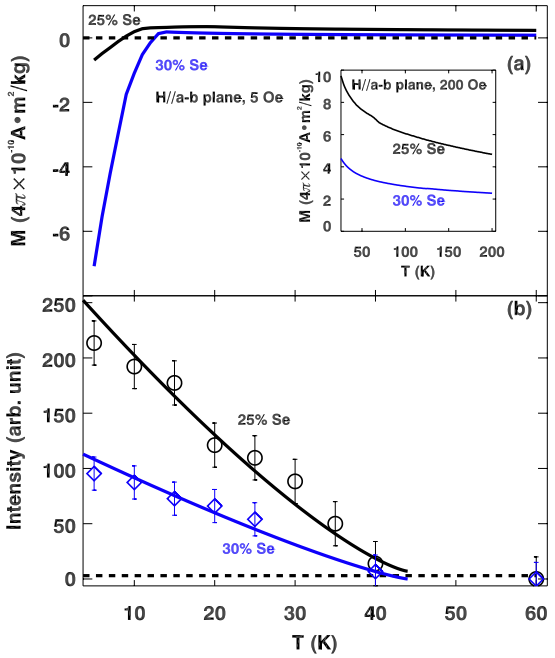

FIG. 1. (Color online) (a) ZFC magnetization and (b) background-subtracted magnetic peak intensity measured along [100] (normalized to the sample mass) as a function of temperature for $Fe_{1.07}Te_{0.75}Se_{0.25}$ and $FeTe_{0.7}Se_{0.3}$. Error bars indicate one standard deviation assuming Poisson statistics. Lines through data are guides for the eyes.

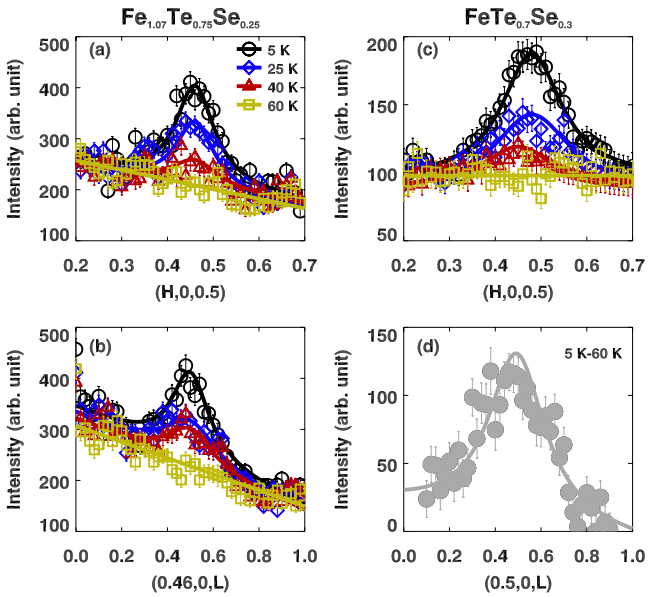

FIG. 2. (Color online) Short-range magnetic order in $Fe_{1+\delta}Te_{1-x}Se_x$. The left and right columns show the magnetic peak profiles for $Fe_{1.07}Te_{0.75}Se_{0.25}$ and $FeTe_{0.7}Se_{0.3}$, respectively. Top and bottom rows are scans along [100] and [001], respectively. (a)–(c) are data taken at various temperatures. For the 30% Se sample, there is a temperature-independent spurious peak in the [001] scans, so in (d) we only plot 5 K data with the 60-K scan subtracted. All data are taken with 1 min counting time and then normalized to the sample mass. Error bars represent the square root of the total counts. The lines are fits to the data using Lorentzian functions.

In our elastic neutron-scattering measurements, each sample was aligned on the (200) and (001) nuclear Bragg peaks with an accuracy and reproducibility in longitudinal wave vector of better than 0.005 r.l.u. For the magnetic peaks, linear scans were performed along [100] and [001] directions at various temperatures. The temperature dependence of the peak intensity is summarized in Fig. 1(b) and representative scans are shown in Fig. 2. No net peak intensity is observed at 60 K, but a weak magnetic peak appears at slightly lower temperature, growing in intensity with further cooling. For $Fe_{1.07}Te_{0.75}Se_{0.25}$, the magnetic structure is clearly incommensurate and the peak position is determined to be $(0.5-\epsilon,0,0.5)$, with $\epsilon=0.04$. From Fig. 2(a), we did not observe a peak at $(0.5+\epsilon,0,0.5)$. For $FeTe_{0.7}Se_{0.3}$, the magnetic peak center is at (0.48,0,0.5), although this differs from the commensurate position by less than the peak width. Our observations are qualitatively consistent with the previous result[23] for $Fe_{1.08}Te_{0.67}Se_{0.33}$, where the magnetic peak is at (0.438,0,0.5); it appears that both the Fe and Se concentrations impact the ordering wave vector. We have also searched for SDW order around (0.5,0.5,0.5) in the (*HHL*) zone, but no evidence of magnetic peaks was found.

At 5 K, the peak width for $Fe_{1.07}Te_{0.75}Se_{0.25}$ [100] scan is 0.10 r.l.u., which corresponds to a correlation length of 6.1(1) Å. The width along [001] is 0.20 r.l.u., giving a correlation length of 4.9(1) Å. As can be seen from Fig. 2, the peaks for $FeTe_{0.7}Se_{0.3}$ along [100] and [001] are broader than their counterparts for $Fe_{1.07}Te_{0.75}Se_{0.25}$ and the correlation lengths are determined to be 3.8(1) Å along [100] and 3.3(1) Å along [001]. Also, from Fig. 1(b), one can see that the magnetic peak intensity for $Fe_{1.07}Te_{0.75}Se_{0.25}$ is always higher than the other one. Although the SDW order is short ranged in both compounds and starts at around the same temperature, ~40 K, the order is apparently stronger in the 25% Se sample.

The magnetic structure of the parent compound $Fe_{1+\delta}Te$ can be described by the schematic diagram in the inset of Fig. 3(a), which is adopted from Refs. 22 and 23. Here the magnetic structure consists of two spin sublattices. The spins in both sublattices are found to be aligned along *b* axis. Within each sublattice, the spins have an antiferromagnetic alignment along *a* and *c* axes and ferromagnetic along the *b* axis. The spins have a small out-of-plane component, but here, for simplicity, we are only considering the components in the *a*-*b* plane. With low excess Fe,[22] this configuration gives rise to magnetic Bragg peaks at the commensurate AFM wave vector (0.5,0,0.5). The extra Fe is considered to reside in the interstitial sites of the Te/Se atoms.[23] With more excess Fe, the ordering wave vector becomes incommensurate, which can be explained by a modulation of the ordered moment size and orientation propagating along the *a* axis.[23] The connection between excess Fe and the transition from commensurate to incommensurate order has been modeled theoretically.[29]

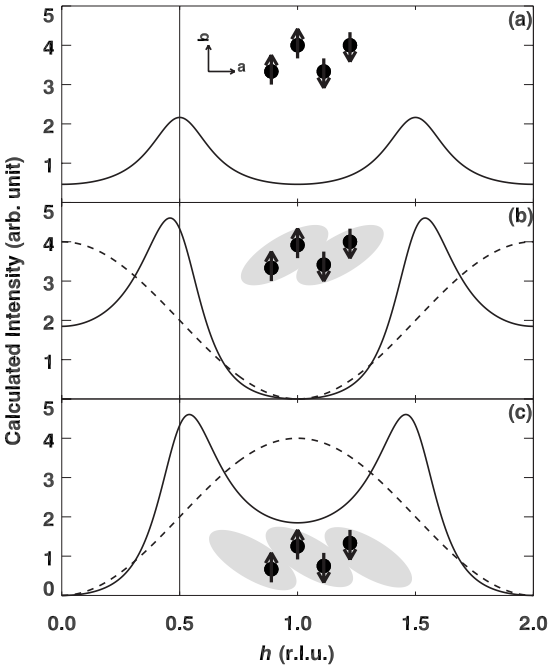

FIG. 3. (a) Inset shows the commensurate magnetic unit cell within a single layer of $Fe_{1+\delta}Te$, with spin arrangements in a-b plane; solid line shows the calculated scattered intensity assuming uniform exponential decay of spin correlations. (b) Dashed line shows the magnetic structure factor $|F|^2$ and solid line shows calculated intensity for exponential decay of correlations between ferromagnetic spin pairs (inset). (c) Same as (b) but for exponential decay of correlations between antiferromagnetic spin pairs.

With Se doping, the magnetic order is depressed and becomes short ranged. It is intriguing that magnetic order can survive without a lowering of the lattice symmetry from tetragonal, although perhaps there are local symmetry reductions on the scale of the magnetic correlation length. The incommensurability is also interesting. A uniform sinusoidal modulation of the spin directions or magnitudes will give incommensurate peaks at $(0.5 \pm \epsilon, 0, 0.5)$, whereas we see a peak only on the $-\epsilon$ side. One can model this with phase-shifted modulations on the two sublattices, but the modulation length required to describe the incommensurability is much greater than the correlation length.

We have found that a simple description of the incommensurability can be obtained when the decay of correlations between ferromagnetic nearest-neighbor spins is different from that of antiferromagnetic spin neighbors. We will consider correlations only along the modulation direction within an a-b plane and assume that they are independent of correlations in the orthogonal directions. Let us break the spin system into perfectly correlated nearest-neighbor pairs, with exponential decay of the spin correlations from one pair to the next along the a axis. The neutron-scattering intensity can then be expressed as[30]

$$I \propto |F|^2 \frac{1-p^2}{1+p^2-2p\cos(2\pi h)}, \tag{1}$$

where F is the structure factor for the selected pair of spins, h is the wave-vector component along the a axis, and

$$p = -e^{-a/\xi}, \tag{2}$$

where p is the correlation function between neighboring pairs, where the negative sign suggests that the interpair correlation is antiferromagnetic, and ξ is the correlation length. (In all cases discussed below, we set $\xi = a$.)

Let us first consider the case of ferromagnetic spin pairs with exponentially decaying correlations between pairs, as illustrated in Fig. 3(b). The structure factor for this case corresponds to

$$|F|^2 = 4\cos^2\left(\tfrac{1}{2}\pi h\right), \tag{3}$$

as indicated by the dashed line in Fig. 3(b). Plugging this into Eq. (1) gives the solid line shown in Fig. 3(b). Note that the calculated peaks are incommensurate, with the peak near $h=0.5$ shifted to lower h. Alternatively, we can start with an antiferromagnetic spin pair, in which case

$$|F|^2 = 4\sin^2\left(\tfrac{1}{2}\pi h\right). \tag{4}$$

This yields the result shown in Fig. 3(c), with the peaks shifted in the opposite direction. If the decay of correlations is identical for ferromagnetic and antiferromagnetic nearest neighbors, then we can average over these two cases, obtaining $|F|^2=2$; the resulting commensurate peaks are shown in Fig. 3(a).

Our experimental results look similar to Fig. 3(b). This suggests that the ferromagnetic correlations are stronger than the antiferromagnetic ones. For the model illustrated in Fig. 3(b), the incommensurability grows as the correlation length gets shorter. The trend in our two samples does not follow this relationship; however, one could describe a more general relationship between the ferromagnetic and antiferromagnetic correlations by taking a weighted average of Eqs. (3) and (4).

In summary, we have observed short-range magnetic order in $Fe_{1.07}Te_{0.75}Se_{0.25}$ and $FeTe_{0.7}Se_{0.3}$. In both samples, the magnetic order is incommensurate and only observed on one side of the commensurate wave vector (0.5,0,0.5), which is likely a result of the imbalance of ferromagnetic/antiferromagnetic correlations between neighboring spins. The parent compound $Fe_{1+\delta}Te$ is not superconducting[22,23] and the optimally doped sample with 50% Se has no static magnetic order.[31,32] Our samples have Se content lying in the middle, where we see that with larger Se doping, the SDW order becomes weaker, while the superconductivity is enhanced. This could imply the coexistence and competition between SDW order and superconductivity in this system, similar to other Fe-based[9,11,13–15] and cuprate superconductors.[33–35] Interestingly, in the $Fe_{1+\delta}Te_{1-x}Se_x$ system, the SDW order and superconductivity can be tuned not only by doping Se, but also by adjusting the Fe content.[20,36,37] It has been reported that the excess Fe acts as a magnetic electron donor,[36] suppresses the superconductivity, and induces a weakly localized electronic state.[38] Our results are completely consistent with these results—with less Fe and more Se, the SDW order is weaker; with more

excess Fe and less Se, superconductivity is weaker, but to really distinguish the role of Fe and Se, samples only varying one element are certainly required for future work. We also note that recent studies of superconducting $FeTe_{0.6}Se_{0.4}$ (Ref. 31) and $FeTe_{0.5}Se_{0.5}$ (Ref. 39) show evidence of a spin gap and resonance peak at the wave vector $(0.5, 0.5, L)$. It should be interesting to study how the magnetic correlations evolve with Se concentration between 30% and 40%.

The work at Brookhaven National Laboratory was supported by the Office of Science, U.S. Department of Energy, under Contract No. DE-AC02-98CH10886.

[1] Y. Kamihara, T. Watanabe, M. Hirano, and H. Hosono, J. Am. Chem. Soc. **130**, 3296 (2008).
[2] H. Takahashi, K. Igawa, K. Arii, Y. Kamihara, M. Hirano, and H. Hosono, Nature (London) **453**, 376 (2008).
[3] X. H. Chen, T. Wu, G. Wu, R. H. Liu, H. Chen, and D. F. Fang, Nature (London) **453**, 761 (2008).
[4] Z.-A. Ren *et al.*, Chin. Phys. Lett. **25**, 2215 (2008).
[5] C. de la Cruz *et al.*, Nature (London) **453**, 899 (2008).
[6] Y. Qiu *et al.*, Phys. Rev. Lett. **101**, 257002 (2008).
[7] Q. Huang, Y. Qiu, W. Bao, M. A. Green, J. W. Lynn, Y. C. Gasparovic, T. Wu, G. Wu, and X. H. Chen, Phys. Rev. Lett. **101**, 257003 (2008).
[8] F. Ma and Z.-Y. Lu, Phys. Rev. B **78**, 033111 (2008).
[9] J. Dong *et al.*, Europhys. Lett. **83**, 27006 (2008).
[10] I. I. Mazin, D. J. Singh, M. D. Johannes, and M. H. Du, Phys. Rev. Lett. **101**, 057003 (2008).
[11] J. Zhao *et al.*, Nature Mater. **7**, 953 (2008).
[12] H. Luetkens *et al.*, Nature Mater. **8**, 305 (2009).
[13] A. J. Drew *et al.*, Nature Mater. **8**, 310 (2009).
[14] M. Rotter, M. Pangerl, M. Tegel, and D. Johrendt, Angew. Chem., Int. Ed. **47**, 7949 (2008).
[15] H. Chen *et al.*, Europhys. Lett. **85**, 17006 (2009).
[16] L. Fang, H. Luo, P. Cheng, Z. Wang, Y. Jia, G. Mu, B. Shen, I. Mazin, L. Shan, C. Ren, and H. Wen, arXiv:0903.2418 (unpublished).
[17] J.-H. Chu, J. G. Analytis, C. Kucharczyk, and I. R. Fisher, Phys. Rev. B **79**, 014506 (2009).
[18] F.-C. Hsu *et al.*, Proc. Natl. Acad. Sci. U.S.A. **105**, 14262 (2008).
[19] K.-W. Yeh *et al.*, Europhys. Lett. **84**, 37002 (2008).
[20] M. H. Fang, H. M. Pham, B. Qian, T. J. Liu, E. K. Vehstedt, Y. Liu, L. Spinu, and Z. Q. Mao, Phys. Rev. B **78**, 224503 (2008).
[21] D. Fruchart, P. Convert, P. Wolfers, R. Madar, J. P. Senateur, and R. Fruchart, Mater. Res. Bull. **10**, 169 (1975).
[22] S. Li *et al.*, Phys. Rev. B **79**, 054503 (2009).
[23] W. Bao *et al.*, Phys. Rev. Lett. **102**, 247001 (2009).
[24] J. Zhao, W. Ratcliff, J. W. Lynn, G. F. Chen, J. L. Luo, N. L. Wang, J. Hu, and P. Dai, Phys. Rev. B **78**, 140504(R) (2008).
[25] T. A. Maier and D. J. Scalapino, Phys. Rev. B **78**, 020514(R) (2008).
[26] Z. P. Yin, S. Lebègue, M. J. Han, B. P. Neal, S. Y. Savrasov, and W. E. Pickett, Phys. Rev. Lett. **101**, 047001 (2008).
[27] F. Ma, W. Ji, J. Hu, Z.-Y. Lu, and T. Xiang, Phys. Rev. Lett. **102**, 177003 (2009).
[28] M. D. Johannes and I. I. Mazin, Phys. Rev. B **79**, 220510(R) (2009).
[29] C. Fang, B. A. Bernevig, and J. Hu, Europhys. Lett. **86**, 67005 (2009).
[30] A. Guinier, *X-Ray Diffraction in Crystals, Imperfect Crystals, and Amorphous Bodies* (Dover, New York, 1994), Chap. 9.
[31] Y. Qiu, W. Bao, Y. Zhao, C. Broholm, V. Stanev, Z. Tesanovic, Y. C. Gasparovic, S. Chang, J. Hu, B. Qian, M. Fang, and Z. Mao, Phys. Rev. Lett. **103**, 067008 (2009).
[32] J. Wen, G. Xu, Z. Xu, G. Gu, and J. M. Tranquada (unpublished).
[33] E. Demler, S. Sachdev, and Y. Zhang, Phys. Rev. Lett. **87**, 067202 (2001).
[34] A. R. Moodenbaugh, Y. Xu, M. Suenaga, T. J. Folkerts, and R. N. Shelton, Phys. Rev. B **38**, 4596 (1988).
[35] B. Lake *et al.*, Nature Mater. **4**, 658 (2005).
[36] L. Zhang, D. J. Singh, and M. H. Du, Phys. Rev. B **79**, 012506 (2009).
[37] T. M. McQueen *et al.*, Phys. Rev. B **79**, 014522 (2009).
[38] T. J. Liu, X. Ke, B. Qian, J. Hu, D. Fobes, E. Vehstedt, H. Pham, J. Yang, M. Fang, L. Spinu, P. Schiffer, Y. Liu, and Z. Mao, arXiv:0904.0824 (unpublished).
[39] H. A. Mook, M. Lumsden, A. Christianson, B. Sales, R. Jin, M. McGuire, A. Sefat, D. Mandrus, S. Nagler, T. Egami, and C. de la Cruz, arXiv:0904.2178 (unpublished).